= 3.0 × 4.0 mm. A total of 3666 reflections had $F > 2.33\sigma(F)$; these were used in the refinement. The limits of data collection were $5° < 2\theta < 50°$.

The structure was solved using conventional Patterson and Fourier techniques. Refinement, using standard full-matrix least-squares cycles, located all atoms including hydrogens. These were refined isotropically while all other atoms were refined anisotropically. Refinement converged at $R(F) = 0.036$, $R_w(F) = 0.038$. The goodness of fit for the last cycle was 1.012, while the maximum $\Delta/\sigma = 0.10$.

1,2-$Mo_2(C_6H_4Me\text{-}4)_2(NMe_2)_4$. The sample used in the study was cleaved from a larger needle and transferred to the goniostat, using standard inert atmosphere handling techniques. Data were collected at -162 °C and yielded the following cell dimensions from a reciprocal-space search: space group = *Pcan*, $a = 8.046$ (2) Å, $b = 17.319$ (7) Å, $c = 18.179$ (8) Å, $V = 2533.2$ Å^3, $Z = 4$, $d_{calcd} = 1.443$ g cm^{-3}, using Mo Kα ($\lambda = 0.71069$ Å), $\mu = 9.802$, scan speed = 4.0 deg min^{-1}, scan width = 2.0 + dispersion, single background at extremes of scan = 5 s, aperture size = 3.0 × 4.0 mm, $5° < 2\theta < 50°$.

Of a total of 3688 reflections, 2250 were unique, and 1864 had $F > 2.33\sigma(F)$; the latter were used in refinement. The structure was solved by direct methods and refined by full-matrix least squares, using isotropic thermal parameters for hydrogens. The structure converged at $R(F) = 0.038$, $R_w(F) = 0.026$, there being no peak greater than 0.42 electron Å^{-3} in the final difference Fourier map. The goodness of fit for the last cycle was 3.397, while the maximum $\Delta/\sigma = 0.05$.

1,2-$Mo_2(C_6H_4Me\text{-}2)_2(NMe_2)_4$. Golden crystals of the titled compound were grown from hexane. A crystal was mounted on the diffractometer as described for the previous structures. Cell dimensions and data were collected at -161 °C and are as follows: space group $A2/a$, $a = 16.845$ (4) Å, $b = 17.651$ (5) Å, $c = 8.451$ (2) Å, $\beta = 102.74$ (1)°, $V = 2451.0$ Å^3, $Z = 4$, $d_{calcd} = 1.492$ g cm^{-3}, using Mo Kα radiation ($\lambda = 0.71069$ Å), $\mu = 10.130$, scan speed = 3.0 deg min^{-1}, scan width = 2.0 + dispersion, single background time at extremes of scan = 5 s, aperture size = 3.0 × 6.0 mm.

The total number of reflections collected was 2568 with $5° < 2\theta < 50°$. Out of 2171 unique intensities, 1892 had $F > 2.33\sigma(F)$; these were used in solving the structure. The position of all atoms was determined by using direct methods and full-matrix least squares. Hydrogen atoms were refined isotropically, while for all other atoms anisotropic thermal parameters were used. Refinement converged at $R(F) = 0.033$, $R_w(F) = 0.023$, with the goodness of fit for the last cycle being 2.981 and the maximum $\Delta/\sigma = 0.05$. A final difference Fourier synthesis was featureless, the largest peak being 0.45 electron Å^{-3}.

Acknowledgment. We thank the Office of Naval Research and the Wrubel Computing Center for support of this work.

Registry No. 1,2-$Mo_2(CH_2Ph)_2(NMe_2)_4$, 82555-51-9; 1,2-$W_2(CH_2Ph)_2(NMe_2)_4$, 82555-52-0; 1,2-$Mo_2(CH_2C_6H_4Me\text{-}4)_2(NMe_2)_4$, 84417-29-8; 1,2-$Mo_2Ph_2(NMe_2)_4$, 84417-24-3; 1,2-$W_2Ph_2(NMe_2)_4$, 84417-25-4; 1,2-$Mo_2(C_6H_4Me\text{-}2)_2(NMe_2)_4$, 84417-23-2; 1,2-$W_2(C_6H_4Me\text{-}2)_2(NMe_2)_4$, 84417-27-6; 1,2-$Mo_2(C_6H_4Me\text{-}4)_2(NMe_2)_4$, 84417-22-1; 1,2-$W_2(C_6H_4Me\text{-}4)_2(NMe_2)_4$, 84417-28-7; 1,2-$W_2(C_6H_2Me_3\text{-}2,4,6)_2(NMe_2)_4$, 84417-26-5; $Mo_2Cl_2(NMe_2)_4$, 63301-82-6; $W_2Cl_2(MMe_2)_4$, 63301-81-5; $C_6H_5CH_2Cl$, 100-44-7; *p*-tolylCH$_2$Cl, 106-43-4; BuLi, 109-72-8; PhLi, 591-51-5; *p*-tolyllithium, 2417-95-0; *p*-tolyl bromide, 106-38-7; benzyllithium, 766-04-1; *o*-tolyllithium, 6699-93-0; mesityllithium, 5806-59-7.

Supplementary Material Available: Tables of observed and calculated structure factor amplitudes and anisotropic thermal parameters for the 1,2-$M_2R_2(NMe_2)_4$ compounds where R = $CH_2C_6H_5$, C_6H_5Me-2, and C_6H_5Me-4 (62 pages). Ordering information is given on any current masthead page.

Protonation Equilibria in Excited-State Tris(bipyrazine)ruthenium(II)

R. J. Crutchley,* N. Kress, and A. B. P. Lever*

Contribution from the Department of Chemistry, York University, Downsview, Ontario, Canada M3J 1P3. *Received June 17, 1982*

Abstract: The tris(bipyrazine)ruthenium(II) cation has six peripheral uncoordinated nitrogen atoms potentially available for protonation in acidic media. Studies of the absorption and emission spectroscopy of the ruthenium cation in media ranging from neutral water to concentrated sulfuric acid show that it is, indeed, possible to sequentially protonate these six nitrogen atoms. As the acidity is increased, a series of isosbestic points are seen in the absorption spectra, and these shift as the equilibria change upon increasing acidity. The parallel studies of emission show six different protonated species with distinct emission maxima and lifetimes ranging from 27 to 520 ns. The first three protonation steps, to three different bipyrazine rings on the cation, have MLCT excited states that are stronger bases than the ground state, while for the second set of three protonation species, the MLCT excited states are weaker bases than the ground state. pK_a and pK_a* values for many of the species are reported. Protonation equilibria with the free base bipyrazine are also included.

During the past 15 years there has been great activity studying the ground- and excited-state chemistry of the $Ru(bpy)_3^{2+}$ cation (I) (bpy = 2,2′-bipyridine). Of particular relevance have been studies of the excited-state photochemistry and photophysics of this species with a view to developing solar energy conversion catalysts. The area is the subject of a recent review.[1] The considerable effort expended on this species has also contributed greatly to our understanding of the chemistry of inorganic molecules in their excited states.

The analogous $Ru(bpz)_3^{2+}$ cation (II) (bpz = bipyrazine) has also been shown[2] to be an excellent photocatalyst, complementary in many ways to species I. In a detailed study of bipyrazine metal complexes,[2] the redox couples were shown, generally, to be shifted ca. 0.5 V positive relative to corresponding couples in corresponding bipyridine complexes. This positive shift was seen to be due to much reduced σ bonding strength in the bipyrazine, relative to the bipyridine derivatives.

Thus the bipyrazine complexes have the potential to be better oxidizing photocatalysts than their bipyridine analogues. There is considerable interest in generating photocatalysts capable of photooxidizing water or halogen ions, hence our continuing interest in these bipyrazine species. The existence of uncoordinated nitrogen atoms on the periphery of species II not only provides a possible mechanism for coupling a substrate molecule to the excited photocatalyst but also, via protonation, can be expected to yield species with even more positive oxidizing potentials.

In this paper, we report spectrophotometric absorption and emission studies performed both on free bipyrazine and on the

(1) Kalyanasundarum, K. *Coord. Chem. Rev.* **1979**, *46*, 159-244.
(2) Crutchley, R. J.; Lever, A. B. P. *J. Am. Chem. Soc.* **1980**, *102*, 7128-7129; *Inorg. Chem.* **1982**, *21*, 2276-2282.

0002-7863/83/1505-1170$01.50/0

ruthenium complex (II) in media from neutral water to 96% sulfuric acid. Analysis of the data leads to the conclusion that bipyrazine undergoes three protonation steps as the acidity is increased while cation II undergoes six protonation steps. Both these systems are quite stable and reversible. Ground-state absorption data lead to derivation of certain of the proton equilibria leading to ground-state pK_a values. Many of the protonated species are luminescent and their emission spectra and lifetimes are reported. These allow determination of some of the excited-state pK_a* values. We demonstrate that for the first three steps, the excited protonation species is a stronger base than the ground state, while the reverse is true for the remaining protonation steps. These results are interpreted in terms of the nature of the excited states involved.

These protonation equilibria are an excellent and unique probe into the excited-state chemistry of these species. Clearly the bipyrazine complex (II) offers a clear advantage in this respect to the bipyridine species (I) which decomposes under similar conditions. However, we note that Demas has reported some interesting protonation equilibria with the species Ru(bpy)$_2$(CN)$_2$,[3] to which we return below.

Experimental Section

Ru(bpz)$_3$Cl$_2$ and bpz were prepared by literature methods.[2] Stock 96% H_2SO_4 (BDH analar grade) was standardized (18.00 ± 0.05 M) by dilution to 0.09 N and titration against 0.1 N NaOH (concentrated BDH volumetric solution), with phenolphthalein as indicator. Doubly distilled water, the last distillation over $KMnO_4$, was used to make up all solutions. Weakly acidic solutions (pH 5–0.5) were made up with 0.1 N HCl (concentrated BDH volumetric solution) instead of 0.1 N H_2SO_4, since possible quenching by HSO_4^- was not desired. No quenching was observed in solutions containing 0.1 M KCl or Na_2SO_4. Fuming H_2SO_4 (15%), used to prepare 97–100% H_2SO_4, was purchased from Fisher Chemicals.

Spectrophotometric Technique. Although Ru(bpz)$_3^{2+}$ and bpz stock solutions in 96% H_2SO_4 appeared stable for months at a time in dark storage, fresh stock solutions were prepared for this study. All spectra were recorded on a Perkin-Elmer Hitachi Model 340 microprocessor spectrometer. The graphical method[4] for determining the number of species in solution requires large absorbance changes to reduce error to a minimum. Where possible, an isosbestic point for a given protonation step was chosen as an origin and the spectrum run with the absorbance scale expanded. Hammett acidities, H_0, were used to calculate pK_a's in concentrated H_2SO_4 solutions.[5-7]

Emission and Lifetime Measurements. Emission spectra were recorded on a Varian SF-330 spectrofluorometer. It is not known whether the reaction rate constant between Ru(bpz)$_3^{2+}$ and H^+ is influenced by the presence of oxygen in solution.[8] This required weakly acidic solutions (pH 5–0.5) to be argon-gassed before measurements were taken. Lifetime measurements of protonated Ru(bpz)$_3^{2+}$ complexes in concentrated H_2SO_4 solutions were independent of atmospheric oxygen in solution and so these solutions were not argon gassed. Emission spectra in Figures 9–11 are uncorrected for variation in phototube sensitivity with wavelength. Excitation wavelengths corresponded to isosbestic points or to wavelengths which required little correction for absorbance changes. Lifetimes measurements were obtained with a 0.5-MW pulsed nitrogen laser (built in the York University workshops) possessing 5-ns pulses at 337 nm. The emission from the various solutions was passed through a monochromator equipped with a filter to remove stray laser radiation. The output from the monochromator was detected by a R928 Hammamatsu photomultiplier and either displayed on a 100-MHz Hewlett Packard oscilloscope or processed through a Princeton Applied Research (PAR) Model 162 boxcar averager with Model 165 gated integrator, prior to display on a PAR series 8002 X-Y Recorder.

Results

Bipyrazine (bpz). Bpz is freely soluble in sulfuric acid and can be recovered unchanged quantitatively therefrom. The spectroscopic data reported here are reversible and reproducible irrespective of whether they are obtained by adding concentrated sulfuric acid to a water solution of bpz or by addition of water to a concentrated sulfuric acid solution of bpz.

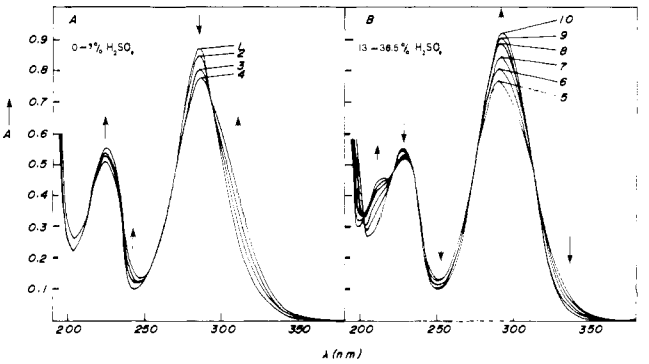

Figure 1. Absorption spectrum of 5.0 × 10^{-5} M bpz in aqueous sulfuric acid solution at ambient temperature as a function of [H_2SO_4]. (A) Curves 1, 2, 3, and 4 correspond to [H_2SO_4] of 0, 1.4, 3.5, and 7.0%, respectively. (B) Curves 5, 6, 7, 8, 9, and 10 correspond to [H_2SO_4] of 13.0, 18.7, 24.1, 29.1, 33.8, and 38.5%, respectively.

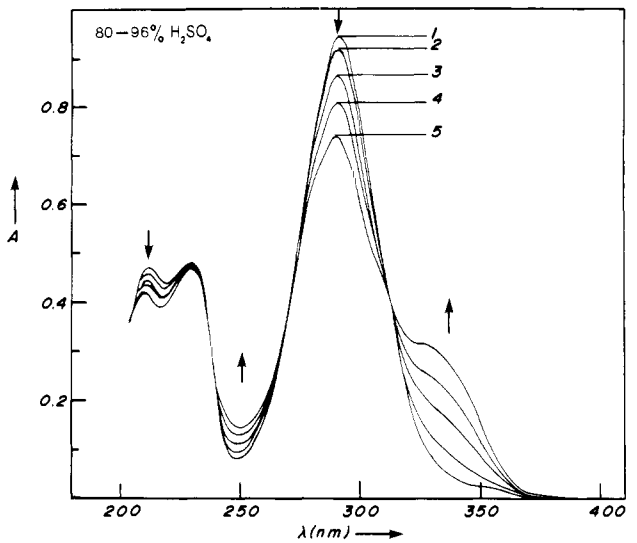

Figure 2. Absorption spectrum of 5.1 × 10^{-5} M bpz in aqueous sulfuric acid solution at ambient temperature as a function of [H_2SO_4]. Curves 1, 2, 3, 4, and 5 correspond to [H_2SO_4] of 80, 89.5, 92.5, 94.2, and 96%, respectively.

Table I. Protonation of Bipyrazine

sulfuric acid concn, %	protonation step	isosbestic points, nm	no. of species	wavelength max, nm
0	0		1	288, 228
1–7	1	297, 256, 217	2	310 sh, 289, 230
7–38.5	2	313, 275, 222, 202	2	294, 230, 214
39–80	2	no significant changes	2	294, 230, 214
80–96	3	315, 274, 240	2	324, 294, 230, 214

The UV absorption spectra in Figures 1 and 2 show the progressive protonation of bpz in 0–96% sulfuric acid. In Figure 1, two sets of isosbestic points suggest two separate protonations of bpz. From 0–7% sulfuric acid, the first set of isosbestic points at 297, 256, and 217 nm appears. The $\pi \rightarrow \pi^*$ band at 289 nm begins to drop in intensity and develops a low-energy shoulder. The $\pi \rightarrow \pi^*$ band at 228 nm actually increases in intensity and is slightly shifted to 230 nm. Increasing the acid concentration further, from 13 to 38.5% sulfuric acid, results in a second set of isosbestic points at 313, 275, 222, and 202 nm. A single $\pi \rightarrow \pi^*$ band at 294 nm is now observed. The $\pi \rightarrow \pi^*$ band at 230 nm has now decreased slightly in intensity and a new band at 214

(3) Peterson, S. H.; Demas, J. N. *J. Am. Chem. Soc.* **1979**, *101*, 6571–6577.
(4) Coleman, J. S.; Varga, L. P.; Mastin, H. *Inorg. Chem.* **1970**, *9*, 1015–1020.
(5) Long, F. A.; Paul, M. A. *Chem. Rev.* **1957**, *57*, 1–45.
(6) Jorgensen, M. J.; Hartter, D. R. *J. Am. Chem. Soc.* **1963**, *85*, 878–883.
(7) Gillespie, R. J.; Peel, T. E.; Robinson, E. A. *J. Am. Chem. Soc.* **1972**, *93*, 5083–5087.
(8) Lasser, N.; Feitelson, J. *J. Phys. Chem.* **1973**, *77*, 1011–1016.

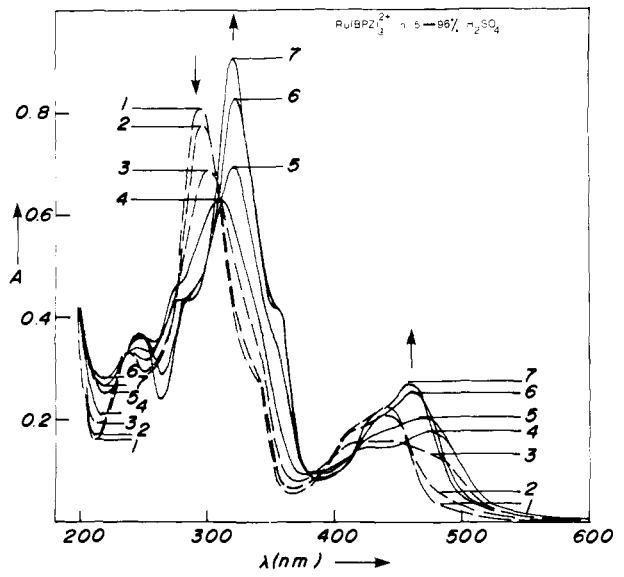

Figure 3. Absorption spectrum of 1.5×10^{-5} M $Ru(bpz)_3^{2+}$ in aqueous sulfuric acid solution at ambient temperature as a function of $[H_2SO_4]$. Curves 1, 2, 3, 4, 5, 6, and 7 correspond to $[H_2SO_4]$ of 5, 24.1, 42.5, 53.2, 66.3, 80.5, and 96%, respectively.

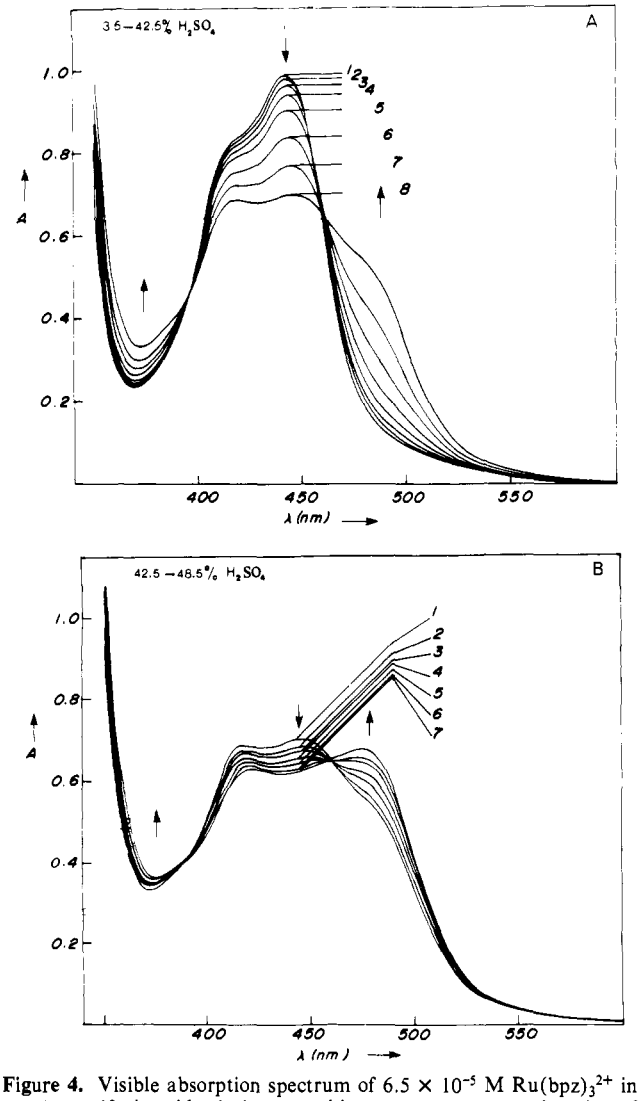

Figure 4. Visible absorption spectrum of 6.5×10^{-5} M $Ru(bpz)_3^{2+}$ in aqueous sulfuric acid solution at ambient temperature as a function of $[H_2SO_4]$. (A) Curves 1, 2, 3, 4, 5, 6, 7, and 8 correspond to $[H_2SO_4]$ of 3.5, 13.0, 18.9, 24.1, 29.1, 33.8, 38.3, and 42.5%, respectively. (B) Curves 1, 2, 3, 4, 5, 6, and 7 correspond to $[H_2SO_4]$ of 42.5, 43.6, 44.6, 45.6, 46.6, 47.5, and 48.5%, respectively.

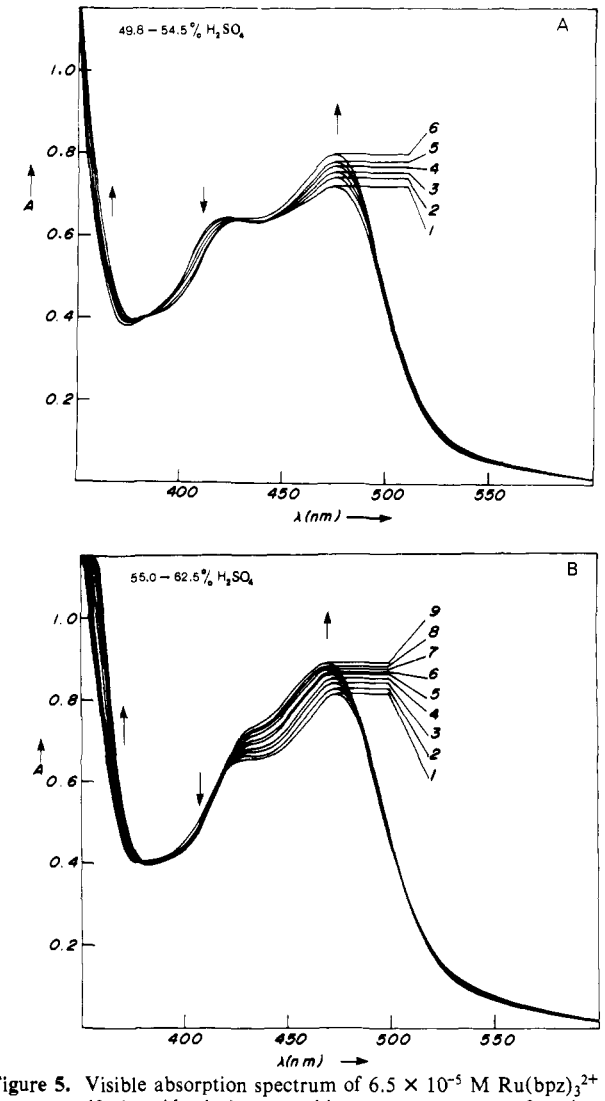

Figure 5. Visible absorption spectrum of 6.5×10^{-5} M $Ru(bpz)_3^{2+}$ in aqueous sulfuric acid solution at ambient temperature as a function of $[H_2SO_4]$. (A) Curves 1, 2, 3, 4, 5, and 6 correspond to $[H_2SO_4]$ of 49.8, 50.4, 51.3, 52.2, 53.2, and 54.5%, respectively. (B) Curves 1, 2, 3, 4, 5, 6, 7, 8, and 9 correspond to $[H_2SO_4]$ of 55.0, 55.8, 56.9, 57.5, 58.3, 59.2, 60, 60.8, 61.6, and 62.5%, respectively.

nm is beginning to appear. From 39 to 80% sulfuric acid, only small absorbance changes are observed in the bpz UV spectrum. However, from 80 to 96% sulfuric acid (see Figure 2), additional protonation results in a third set of isosbestic points at 315, 274, and 240 nm. The $\pi \rightarrow \pi^*$ bands centered at 294, 230, and 214 nm drop in intensity while a new band begins to appear at approximately 324 nm. Protonation is, however, incomplete in 96% sulfuric acid. These data are summarized in Table I.

$Ru(bpz)_3^{2+}$ (II). The ruthenium complex can be recovered quantitatively and unchanged from concentrated sulfuric acid, and as noted for bpz itself, the data are independent of whether they are collected by increasing or decreasing the acidity. Solutions of species II in concentrated sulfuric acid appear indefinitely stable in the dark.

In Figure 3, the overall effects upon the UV and visible spectrum of II are shown as the medium changes from 5–96% sulfuric acid. As the acidity increases, the low-energy $\pi \rightarrow \pi^*$ band at 294 nm decreases in intensity and red shifts, reaching a minimum at 310 nm in 53.2% sulfuric acid. A further increase in acidity increases the intensity of this band until it reaches a new maximum at 318 nm in 96% sulfuric acid.

When the data are collected in a stepwise fashion, isosbestic points not obvious in Figure 3 can be observed. Thus, in Figures 4–6 are shown the stepwise changes in absorption spectra as the acidity is increased by raising the sulfuric acid concentration.

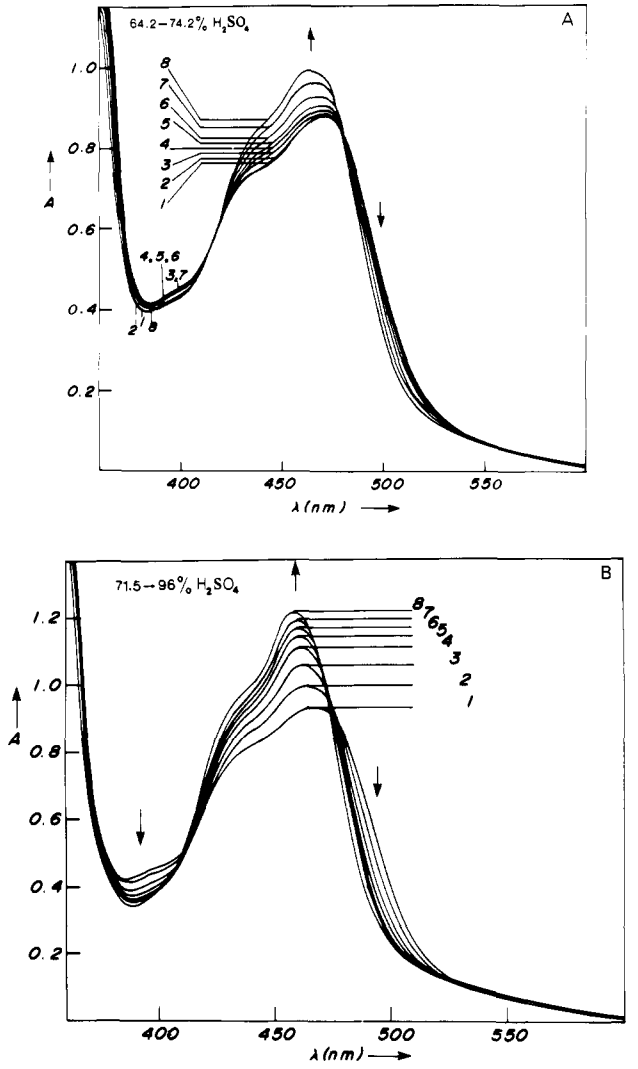

Figure 6. Visible absorption spectrum of 6.5×10^{-5} M $Ru(bpz)_3^{2+}$ in aqueous sulfuric acid solution at ambient temperature as a function of $[H_2SO_4]$. (A) Curves 1, 2, 3, 4, 5, 6, 7, and 8 correspond to $[H_2SO_4]$ of 64, 65.5, 67, 68.5, 70, 71.5, 73, and 74.3%, respectively. (B) Curves 1, 2, 3, 4, 5, 6, 7, and 8 correspond to $[H_2SO_4]$ of 71.5, 74.3, 77, 79.5, 82.5, 85, 88, and 96%, respectively.

Under these circumstances, series of isosbestic points are formed in specific acidity regions, then decay, to be replaced by new sets of isosbestic points. We persue, in particular, the changes in the 300–700-nm region where the ruthenium to ligand MLCT transitions are observed. Each figure represents a significant change in isosbestic points as protonation proceeds. In Figure 4A (3.5–42.5% sulfuric acid), a slight red shift of the band at 441 nm is followed by a decrease in intensity and the growth of a low-energy shoulder at 475 nm. Isosbestic points appear at 397 and 461 nm. In Figure 4B (42.5–48.5% sulfuric acid), a significant shift in isosbestic points occurs to 389 and 459 nm. The low-energy shoulder at 475 nm has increased its intensity to become a distinguishable band. In Figure 5A (49.8–54.5% sulfuric acid), a new set of isosbestic points appears at 382 and 440 nm. The MLCT band maximum is located at 475 nm with a high-energy shoulder at 426 nm. Interestingly, the MLCT band resembles the MLCT band of $Ru(bpz)_3^{2+}$ in neutral solution except for a considerable broadening, suggesting a lifting of degeneracy of π^* energy levels. In addition, 53.2% sulfuric acid not only corresponds to the maximum concentration of acid in Figure 5A just before a change in isosbestic points but also the $\pi \rightarrow \pi^*$ band minimum at 310 nm in Figure 3. In Figure 5B (55.0–62.5% sulfuric acid), a slight blue shift, narrowing and increasing in intensity, is observed for the MLCT band. New isosbestic points appear at 417 and 379 nm with band maximum at 470 nm. In Figure 6A

Table II. Protonation of $Ru(bpz)_3^{2+}$

sulfuric acid concn, %	protonation step	isosbestic points, nm	no. of species	wavelength max, nm
0	0		1	415 sh, 441
3.5-42.5	1	397, 461	2	415 sh, 445, 475 sh
42.5-48.5	2	389, 459	2	415, 475
49.8-54.5	3	382, 440	2	426, 475
55.0-62.5	4	379, 417	3	430 sh, 470
64.2-74.2	5	415, 482	3	420 sh, 465
71.5-96	6	413, 475	2	430 sh, 458

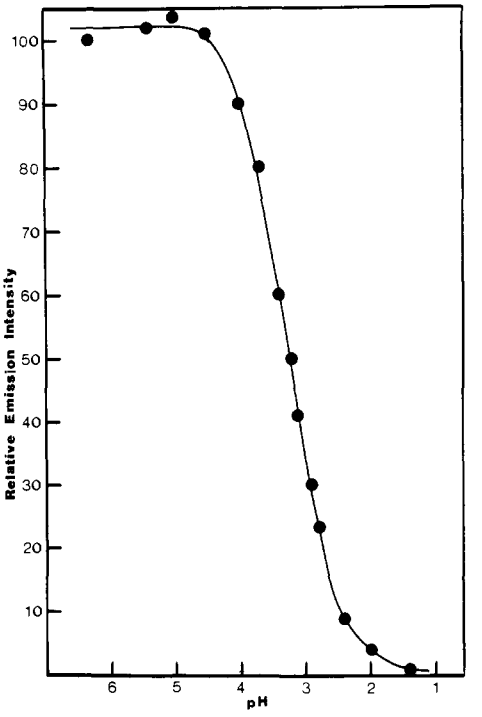

Figure 7. Luminescence titration curve of 1.8×10^{-6} M $Ru(bpz)_3^{2+}$ at ambient temperature in argon-gassed solutions made acidic (pH 6–1) with HCl. Excitation and emission wavelengths set at 429 and 595 nm, respectively.

(64.2–74.2% sulfuric acid), the blue shift, narrowing and increasing in intensity, is continued to be observed for the MLCT band. Isosbestic points appear at 482 and 415 nm with a new band maximum at 465 nm. Between 380 and 410 nm the absorbance changes are not consistent, suggesting a number of subtle changes in the chemistry of the protonated species in solution. In Figure 6B (71.5–96% sulfuric acid), a further blue shift, narrowing and increasing in intensity, is observed for the MLCT band. New isosbestic points appear at 475 and 413 nm with a new band maximum at 458 nm in 96% sulfuric acid. A 2-nm blue shift in the position of the MLCT band continues going from 96% sulfuric acid to 15% fuming sulfuric acid with no increase in intensity. The data are summarized in Table II.

Emission Spectra. In a previous study,[2] we observed that the characteristic emission of species II near 595 nm (uncorrected) is quenched as the acidity is increased. Figure 7 shows the sigmoidal curve obtained as the emission intensity is followed with decreasing pH. However, if the acidity is increased further, emission is recovered, presumably from another species, and a new sigmoidal curve maximizes at 100% sulfuric acid (Figure 8). A careful study of the emission spectra followed over the same acid region makes it evident that several emitting species are involved. Thus, as shown in Figure 9A,B, the initial emission peak at 595 nm weakens, but as it is quenched, new weak luminescence is observed at 717 nm. Subsequent Figures 10 and 11 show that this band red shifts and decreases in intensity and then, as acidity increases further, blue shifts and increases markedly in intensity;

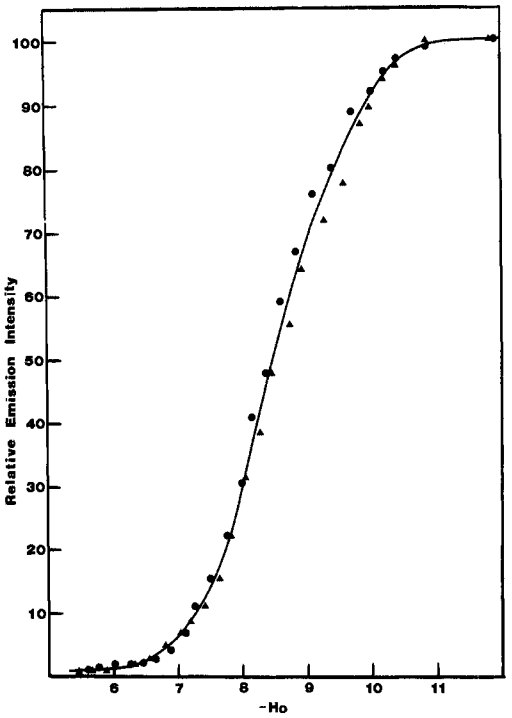

Figure 8. Luminescence titration curve of 1.7×10^{-6} M $Ru(bpz)_3^{2+}$ at ambient temperature in aqueous sulfuric acid solutions (68.5–100% H_2SO_4), with excitation wavelengths at 475 nm (●) or 413 nm (▲) and emission wavelength set at 620 nm.

that several different species are involved is evident from the fact that the peak maxima of these various spectra at different acidities also have different lifetimes as shown in Table IV. We show below that these various species correlate with changes in absorption spectra.

Discussion

Before discussing these data in detail, the remarkable stability of both bpz and its ruthenium complex (II) in concentrated sulfuric acid should be noted. The ability to recover these species unchanged enables us to exclude any irreversible chemical changes from having taken place. In particular, we exclude sulfonation as an explanation for the spectroscopic observations. While under some circumstances sulfonation is reversible, it is unlikely to occur at these highly positive charged species and the quantitative reproducibility and reversibility of these data render it improbable. We continue the discussion on the assumption that the chemical species in solution are unchanged during these experiments, save for varying degrees of protonation ion pairing and possible solvation.

Bipyrazine (bpz). The spectral changes observed between 0 and 96% sulfuric acid are entirely consistent with the effects of protonation on bpz. The observed red shift of the $\pi \rightarrow \pi^*$ bands can be interpreted simply by the stabilization of π^* orbitals through protonation as observed with bipyridine.[9] The large separation between the second and third protonation steps for bpz is paralleled by pyrazine whose acidity constants are $pK_{a_1} = 0.65$ and $pK_{a_2} = -6.25$.[10] Obviously, protonation of an already proton-deactivated pyrazine ring is difficult.

A graphical analysis can be used to determine the number of species in solution from spectrophotometric data.[4] If the absorbance value of a particular solution, j, at a specific wavelength, i, is denoted by A_{ij}, a plot of $A_{ij} - A_{ij'}$ at wavelength i vs the corresponding difference $A_{i'j} - A_{i'j'}$ at another wavelength i' will give a straight line passing through the origin for each i' if only two species exist in solution. When the two sets of absorbance data associated with Figure 1A,B are treated with the above analysis, two straight lines passing through the origin can be obtained. Therefore, we conclude that absorbances changes as-

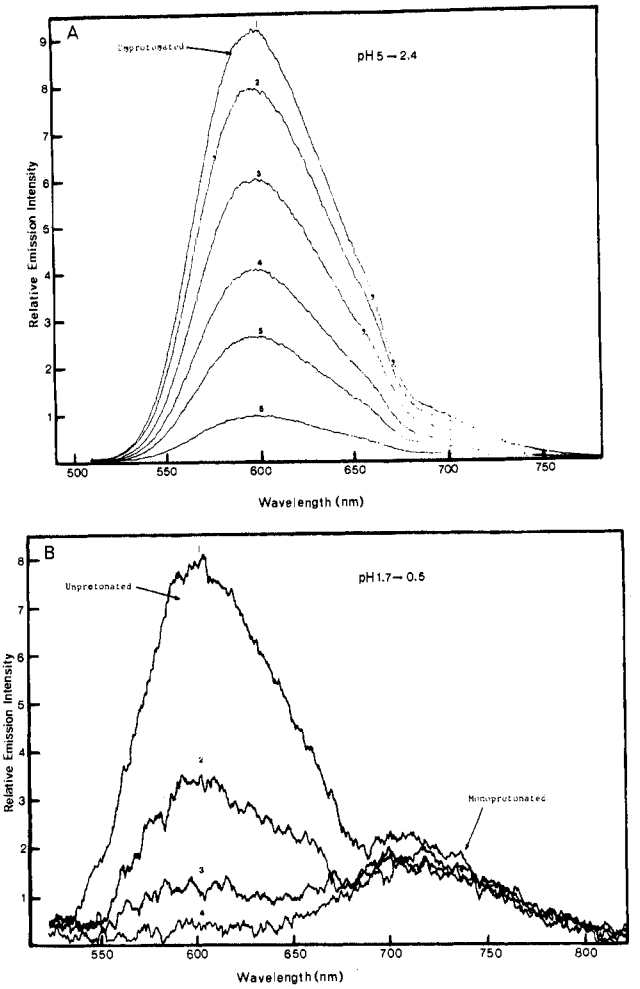

Figure 9. Uncorrected emission spectra of $Ru(bpz)_3^{2+}$ at ambient temperature in argon-gassed aqueous solutions made acidic with HCl. (A) 1.8×10^{-6} M $Ru(bpz)_3^{2+}$. Curves 1, 2, 3, 4, 5, and 6 correspond to pH's of 5, 3.7, 3.4, 3.1, 2.9, and 2.4, respectively. (B) 2.6×10^{-6} M $Ru(bpz)_3^{2+}$. Curves 1, 2, 3, and 4 correspond to pH's 1.7, 1.4, 1.1, and 0.5, respectively. Excitation wavelength set at 429 nm.

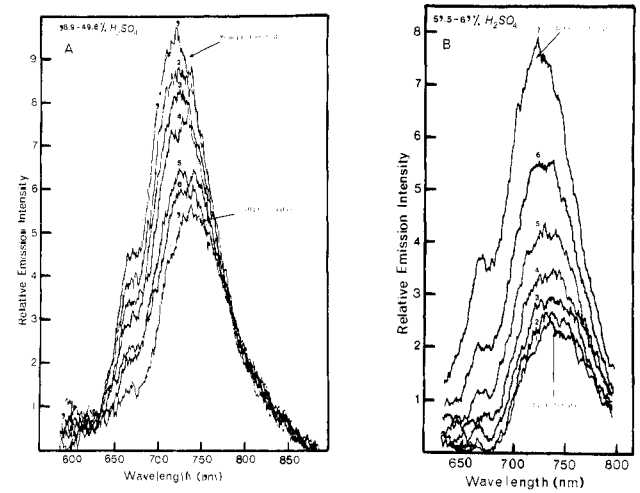

Figure 10. Uncorrected emission spectra of 1.4×10^{-5} M $Ru(bpz)_3^{2+}$ at ambient temperature in aqueous sulfuric acid solutions as a function of $[H_2SO_4]$. (A) Curves 1, 2, 3, 4, 5, 6, and 7 correspond to $[H_2SO_4]$ of 18.9, 29.1, 33.8, 36.1, 40.4, 42.5, and 49.8%, respectively. Excitation wavelength set at 461 nm. (B) Curves 1, 2, 3, 4, 5, 6, and 7 correspond to $[H_2SO_4]$ of 57.5, 59.2, 60.8, 62.5, 64, 65.5, and 67%, respectively. Excitation wavelength set at 413 nm.

(9) Nakamoto, K. *J. Phys. Chem.* **1960**, *64*, 1420–1425.
(10) Brignell, P. J.; Johnson, C. D.; Katritzky, A. R.; Shakir, N.; Tarhan, H. O.; Walker, G. *J. Chem. Soc. B* **1967**, 1233–1235.

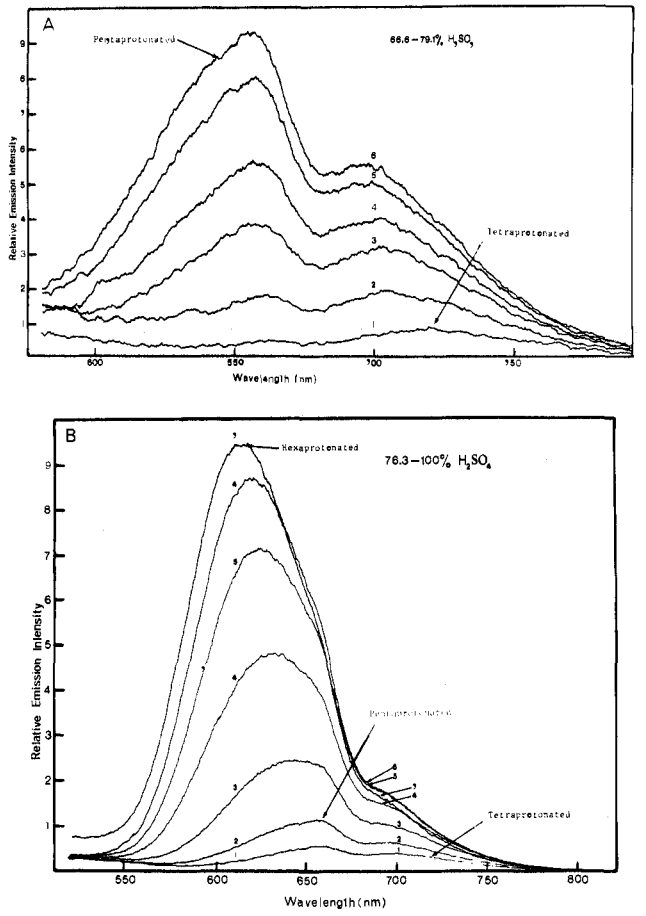

Figure 11. Uncorrected emission spectrum of 1.7×10^{-6} M Ru(bpz)$_3^{2+}$ at ambient temperatures in aqueous sulfuric acid solutions as a function of [H_2SO_4]. (A) Curves 1, 2, 3, 4, 5, and 6 correspond to [H_2SO_4] of 68.5, 73, 75.6, 77, 78.4, and 79.1%, respectively. Excitation wavelength set at 413 nm. (B) Curves 1, 2, 3, 4, 5, 6, and 7 correspond to [H_2SO_4] of 76.3, 79.1, 82.5, 86.5, 91, 96, and 100%, respectively. Excitation wavelength set at 475 nm.

sociated with the first two sets of isosbestic points represent two separate protonation steps. Because the protonation steps occur so close together, it was not possible to draw good sigmoidal curves to determine pK_a, and so the acidity at which the rate of change in absorbance is greatest was chosen to calculate the pK_a for the respective protonation step. In this way, we find pK_{a_1} = 0.45 and pK_{a_2} = −1.35 compared with pK_{a_1} = 4.45[9] and pK_{a_2} = 0.52[11] for bipyridine. Note that pK_{a_1} refers to the monoprotonated species (see Table III). The large separation between pK_{a_1} and pK_{a_2} for bipyridine is thought to be caused by electrostatic repulsion.[11] The absorbance changes associated with the third set of isosbestic points (80–96% sulfuric acid) also give a straight line passing through the origin for the graphical test for two species in solution. Therefore, we are observing the third protonation involving triply protonated bpz with an estimated pK_{a_3} of approximately −10. From 0 to 96% sulfuric acid, protonation is consistent with Scheme I. On the basis of the UV spectrophotometric study of acidic bipyridine solutions,[9] the configurations chosen in Scheme I reflect the need to stabilize a positive charge and reduce the repulsion of like charges. As seen in Figures 1 and 2, bpz exhibits at least two bands in the ultraviolet region. This is an indication that the twist along the central bond is small, since it is shown both empirically[11] and theoretically[12] that for a large twist only one band is usually observed in this region.

Ru(bpz)$_3^{2+}$ Cation. (a) Absorption Spectra. The Ru(bpz)$_3^{2+}$ cation has six aromatic uncoordinated nitrogen atoms potentially

Scheme I

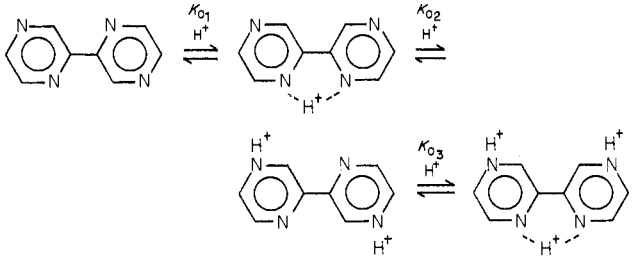

available for protonation. With the exclusion of any net chemical change, the observed spectroscopic behavior with changing acidity must arise from protonation possibly modified by solvatochromic effects. Furthermore, although at intermediate acidity values the absorption emission spectra markedly differ from that of species II in neutral aqueous medium, in concentrated sulfuric acid the supposed hexaprotonated species has absorption (especially the MLCT absorption band) and emission characteristics quite similar to those in neutral medium. This suggests that the excited states in concentrated sulfuric acid and at pH 7 do not differ so much. These similarities are unlikely to occur if coordinated bpz is grossly altered by some chemical reaction or there is loss of coordinated ligand.

Solvatochromic effects have been observed to shift MLCT bands of M(CO)$_4$bpy (M = Mo and W) as much as 47 nm.[13] On the other hand, the visible MLCT band of Fe(bpy)$_3^{2+}$ shifts negligibly in solutions with considerable variation in polarity.[14] Similarly, the position of the visible MLCT band of Ru(bpy)$_3^{2+}$ remains unchanged in solutions of 0–96% sulfuric acid. When this is considered together with the UV spectra of bpz in 0–96% sulfuric acid which demonstrates no unusual spectral changes[15,16] that cannot be ascribed to protonation, it seems unlikely the spectra of Ru(bpz)$_3^{2+}$ over the same acid range will be much influenced by solvatochromic effects.

Instead of invoking unusual and unsupported chemical reactions, protonation provides the most simple and most believable explanation of the spectrophotometric changes observed in Figures 3–6. Consider first how protonation may be expected to influence the visible absorption spectrum of species II.

Although there is some controversy concerning the detailed nature of the absorption features in the visible spectrum of the Ru(bpy)$_3^{2+}$ cation,[1] it is clear that they arise from metal to ligand electron transfer (MLCT) from ruthenium d^6 to ligand π^* orbitals. The same assuredly holds true for the bpz analogue (II).

In the discussion which follows, we develop a protonation model for bpz by using prior studies with bipyridines as a guide. In one model,[17] three bpz π^* levels (one from each bpz ligand in II) couple in D_3 symmetry, to yield $A_2 + E$ molecular orbitals, the latter lying to lower energy. Transitions from the filled $(t_{2g})^6$ level of Ru(II) to these two orbitals, namely $^1E \leftarrow {}^1A_1$ and $^1A_2 \leftarrow {}^1A_1$, are then responsible for the characteristic visible absorption. These transitions may both be represented by Ru(II)d$^6(\pi^*)^0 \rightarrow$ Ru(III)d$^5(\pi^*)^1$.

When the system is monoprotonated, the bpz ligand carrying the proton becomes different from those which do not, and the D_3 symmetry is reduced to C_1. The degeneracy of the E π^* level is lifted. Grossly we expect broadening of the spectrum. The positive charge on coordinated Hbpz$^+$ increases the π acceptor character of the ligand by lowering the π^* energy level and facilitating overlap with ruthenium. The MLCT transition to this specific ligand will then be red shifted relative to the MLCT transition to unprotonated bpz. Previous work with the bipyridine cation (I) has revealed[18] that the excited electron is probably

(11) Westheimer, F. H.; Benfey, O. T. *J. Am. Chem. Soc.* **1956**, *78*, 5309–5311.
(12) Susuki, H. *Bull. Chem. Soc. Jpn.* **1959**, *32*, 1340, 1350, 1357–1361.
(13) Burgess, J. *J. Organomet. Chem.* **1969**, *19*, 218–220.
(14) Burgess, J. *Spectrochim. Acta, Part A* **1970**, *26A*, 1369–1374.
(15) Cox, R. A.; Yates, K. *Can. J. Chem.* **1981**, *59*, 1560–1567.
(16) Campbell, H. J.; Edwards, T. J. *Can. J. Chem.* **1960**, *38*, 2109–2116.
(17) Kober, E. M.; Meyer, T. J. *Inorg. Chem.* **1982**, *21*, 3967–3977.
(18) Bradley, P. G.; Kress, N.; Hornberger, B. A.; Dallinger, R. F.; Woodruff, W. H. *J. Am. Chem. Soc.* **1981**, *103*, 7441–7446.

localized on the bipyridine ligand in the MLCT excited state, for a period of time exceeding several vibrations. Assuming this to be the case here, then we would expect to see a low-energy band corresponding to the transition to the protonated bpz and higher-energy bands corresponding to transitions to the unprotonated bpz. Thus the absorption band should red shift and broaden.

As the second and third protons are added, to each remaining bpz ligand, no further red shifting will occur if each ligand is behaving fairly independently of the others; however, the intensity distribution will shift to the red such that in the triprotonated species, the peak maximum in the broadened absorption will be red shifted relative to the monoprotonated case. Note that the addition of the second, third, fourth, or fifth proton will not give rise to higher symmetry species since, under the Frank–Condon conditions of the excitation, at least one of the protonated bpz ligands is asymmetric. Moreover, there will be several different isomeric forms of the polyprotonated species, depending upon the relative positions of the protons, contributing to the broadness of the transition.

The postulate of a localized protonated bpz ligand in the excited state also allows one to predict that the monoprotonated excited state is a weaker acid than the ground state in that, in this excited state, the bpz ligand is carrying an extra negative charge. This is also consistent with the lowering in energy of the π^* orbital and the red shift in the excitation maximum according to the Forster treatment.[19] By similar arguments the second and third protonated species are also likely to be weaker acids than the ground-state analogues.

The fourth proton must be added to a bipyrazine ligand which already carries one proton. It is more difficult to predict unequivocally the effect of such double protonation. However, the presence of the first proton on the ligand will certainly inhibit binding the second because of their mutual repulsion. Moreover, a doubly protonated H_2bpz^{2+} should be a very poor σ donor ligand; indeed, it is a weak σ donor in its unprotonated form.[2] The high stability of the $Ru(bpz)_3^{2+}$ cation in strong acid must then arise through significant π back-donation, facilitated by the double protonation. While such double protonation should stabilize even further, the ligand π^* orbitals, the coupling between the ruthenium d orbitals, and ligand π^* orbitals, i.e., the magnitude of the off-diagonal matrix element $\langle Ru\ d^6{:}H{:}bpz\ \pi^* \rangle$ may now be so large that the mixed Ru/bpz π^* MLCT excited-state energy is blue shifted relative to the monoprotonated species (e.g., see arguments in ref 20).

By use of the Forster argument,[19] such a blue shift will ensure that the second protonated bpz is a stronger acid in the MLCT excited state than in the ground state. This fact may also be rationalized by the view that, in the monoprotonated excited-state fragment Ru^{III}–Hbpz, extra electron density on the ligand is probably associated with the protonated ring, leaving the unprotonated ring being formally bound to Ru(III) and hence the nitrogen therein is a weaker base than in the ground state bound to Ru(II).

These arguments are supported by Resonance Raman data for $Ru(bpy)_3^{2+}$ which[18] show that the MLCT state is localized on one ring for a lifetime (maximum about 1 ns) certainly long enough to reach protonation equilibrium, if a similar effect is observed here. Wrighton and co-workers[21] have used similar arguments to explain the enhanced acidity of ruthenium(II) complexes of 4,7-dihydroxy-1,10-phenanthroline in the excited state.

As we develop below, these predictions are seen to be accurate and provide additional evidence for our belief that, indeed, six protonation steps can be observed as the acidity of a solution of species II is increased.

Thus, Figures 4A,B and 5A show a series of isosbestic points which grow and then shift as the acidity is increased. Graphical analysis using the two species plot gives a straight line passing through the origin for each set of absorbance data associated with Figures 4A,B and 5A. We, therefore, associate these figures with the first three protonation steps. As predicted above, there is broadening and an initial red shift (Figure 4A) followed by a redistribution of the absorption intensity toward the red but with no further red shift. pK_a values were calculated from the acidity at which the greatest change in absorbance occurred and are reported in Table III. Note that pK_{a_1} for complex II is more negative than the value for the free ligand, indicating that the coordinated bpz is a weaker base than the free ligand. This is contrary to early work by Taube[22] on pyrazine coordinated to Ru(II) but probably arises because there are six nitrogen atoms to share back-donation from the Ru(II) atom.

Table III. Acid Dissociation Constants pK_a and pK_a^*

	protonation steps					
	1	2	3	4	5	6
bpz	0.45	−1.35	?	?		
$Ru(bpz)_3^{2+}$ ground state	−2.2	−3.0	−3.5	?	?	−6.7
excited state[a]	2.0	−2.4	?	?	?	−7.9
calcd excited state[b]	3.8	−2.2	?	?	?	−8.6

[a] pK_a^* from lifetime of equilibrated species in Table IV and eq 1. [b] Calculated pK_a^* from emission maximum in Table IV and eq 2, with T 298 °C.

Scheme II

$$Ru(bpz)_3^{2+} \overset{K_{a_1}}{\underset{H^+}{\rightleftharpoons}} Ru(bpz)_2(Hbpz)^{3+} \overset{K_{a_2}}{\underset{H^+}{\rightleftharpoons}} Ru(bpz)(Hbpz)_2^{4+} \overset{K_{a_3}}{\underset{H^+}{\rightleftharpoons}} Ru(Hbpz)_3^{5+} \overset{K_{a_4}}{\underset{H^+}{\rightleftharpoons}} Ru(Hbpz)_2(H_2bpz)^{6+} \overset{K_{a_5}}{\underset{H^+}{\rightleftharpoons}} Ru(Hbpz)(H_2bpz)_2^{7+} \overset{K_{a_6}}{\underset{H^+}{\rightleftharpoons}} Ru(H_2bpz)_3^{7+}$$

Figures 5B and 6A,B also show the appearance and disappearance of isosbestic points as the acidity continues to increase, but the changes are smaller. Nevertheless, when the variation in emission spectra is considered, it seems clear that a further three protonation steps are, indeed, involved. As protons are added (Figures 5B and 6A,B) the spectrum shifts back to the blue and becomes more narrow. Indeed, the half-bandwidth varies from 3575 cm^{-1} in neutral medium, through 6025 cm^{-1} in the triprotonated form (Figure 5A) back to 3350 cm^{-1} in the supposedly hexaprotonated form in concentrated sulfuric acid (Figure 6B). Graphical analysis, as above, for Figure 5B fails to give a straight line for the two-species plot. However, the test for three species in solution is positive since plots of $(A_{2j} - A_{2j'})/(A_{1j} - A_{1j'})$ vs. $(A_{3j} - A_{3j'})/(A_{1j} - A_{1j'})$ give a straight line for each j' where 1, 2, and 3 are different wavelengths and j' is a specific solution. Unfortunately, the small absorbance changes in Figure 5B and the large associated error suggest the limits of this analysis have been reached. The three species which exist in equilibrium are presumably the tri-, tetra-, and pentaprotonated $Ru(bpz)_3^{2+}$. The absorbance data associated with Figure 6A also fit the three species graphical test, suggesting tetra-, penta-, and hexaprotonated $Ru(bpz)_3^{2+}$ exist in solution. However, it should be noted, the absorbance changes between 380 and 410 nm in Figure 6A are not consistent. The spectrum of $Ru(bpz)_3^{2+}$ in 74.2% sulfuric acid corresponds to the changeover from Figure 6A to the new set of isosbestic points shown in Figure 6B. At 74.2% sulfuric acid, all the tetraprotonated species has been converted to pentaprotonated $Ru(bpz)_3^{2+}$. This is confirmed by the graphical test for two species under conditions of constant stoichiometry for the absorbance changes associated with Figure 6B. Again, the points lie in a straight line through the origin, proving only penta- and hexaprotonated $Ru(bpz)_3^{2+}$ exist in solution.

Since the fourth and fifth protonations overlap to a great extent, a computer analysis is necessary to calculate with any accuracy

(19) Ireland, J. F.; Wyatt, P. A. H. *Adv. Phys. Org. Chem.* **1976**, *12*, 131–221.
(20) Lever, A. B. P.; Ozin, G. A. *Inorg. Chem.* **1977**, *16*, 2012–2016.
(21) Giordano, P. J.; Bock, C. R.; Wrighton, M. S. *J. Am. Chem. Soc.* **1978**, *100*, 6960–6965.
(22) Ford, P.; Rudd, De F. P.; Gaunder, R.; Taube, H. *J. Am. Chem. Soc.* **1968**, *90*, 1187–1194.

Table IV. $Ru(bpz)_3^{2+}$ Cation: Excited-State Emission Wavelength and Lifetimes in Acidic Media

	protonation steps						
	0	1	2	3	4	5	6
emission wavelength, nm	595	717	738	738	720	656	620
lifetime, ns	900	50	27	43	35	130	520
excitation max, nm	423	423	484	484	480	470	467
$[H_2SO_4]$, %	0	18.9	49.8	57.5	68.5	79	100

pK_{a_4} and pK_{a_5}. However, the sixth protonation is separate enough to calculate pK_{a_6}. On the basis of the acid strength at which the greatest change in absorbance occurs, $pK_{a_6} = -6.7$.

The six protonation steps of $Ru(bpz)_3^{2+}$ in 0–96% sulfuric acid are illustrated in Scheme II. Each of the first three protonation steps occur at a separate ligand so that at the completion of the third protonation, each ligand is monoprotonated. Further protonation proceeds on the unprotonated pyrazine moiety of each bpz ligand. There are, possibly, a number of isomers in equilibrium with each other during the protonation steps. The isomers which are expected to be the most stable are those with the greatest separation of charge.

(b) Emission Spectra. In a previous study,[2] we found $Ru(bpz)_3^{2+*}$ emission intensity to decrease at lower acid concentrations than required to monoprotonate $Ru(bpz)_3^{2+}$ in the ground state. The suggested quenching mechanism, protonation of one of the six available aromatic nitrogens as a consequence of the enhanced basicity of MLCT excited state, has been used to explain the pH-dependent emission of some ruthenium bipyridine[23] and bipyrimidine[24] complexes. Figures 9–11 show the uncorrected emission spectra of $Ru(bpz)_3^{2+}$ and its protonated derivatives in aqueous acid solutions from pH 5 to $H_0 = -11.9$. The changes observed in the emission spectra suggest a number of emitting species exist in solution depending on the acid concentration. Since there exist in the ground state a number of protonation equilibria, so the excited state must also be involved in protonation equilibria. In Figure 9A, the emission intensity decreases consistently as acidity increases, suggesting a simple Stern–Volmer quenching mechanism. However, in still greater acidity, Figure 9B shows that while the emission band centered at 595 nm decreases to zero intensity, a new emission band centered at 717 nm persists. This is strong evidence of an excited-state equilibrium between $Ru(bpz)_3^{2+*}$ and $Ru(bpz)_2(Hbpz)^{3+*}$. The emission at 717 nm in aqueous acidic solution (pH 0.5) is approximately 260 times less intense than the emission at 595 nm in aqueous solution at pH 5, neglecting correction for phototube sensitivity (red-sensitive phototube used). The excitation spectra of the 717-nm species and, indeed, of all the emission species reported here (Table IV) are centered around the MLCT band near 450 nm, essentially eliminating the possibility that some of the emission may arise from impurities. It should, therefore, be possible to calculate the excited-state pK_a^* by using eq 1[19,25] where pH is taken at the

$$pK_a^* = \text{pH (or } H_0) + \log (\tau_a/\tau_b) \quad (1)$$

inflection point in the luminescence titration curve (see Figure 7) and τ_a and τ_b are the excited-state lifetimes of protonated and unprotonated forms, respectively (see Table IV). Substituting these values into eq 1 gives $pK_{a_1}^* = 2.0$. Since $pK_{a_1} = -2.2$, the basicity of the excited state has been enhanced by 4.2 pH units relative to the ground state. Forster[26] and later Weller[27] suggested the molar enthalpy, ΔH^*, of the reaction in the excited state differs from the analogous molar enthalpy, ΔH, in the ground state by an amount which is given by the frequency interval, $\Delta\nu$, between the long-wavelength absorption bands of base and acid forms.

(23) Giordano, P. J.; Bock, C. R.; Wrighton, M. S.; Interrante, L. V.; Williams, R. F. X. *J. Am. Chem. Soc.* **1977**, *99*, 3187–3189.
(24) Hunziger, M.; Ludi, A. *J. Am. Chem. Soc.* **1977**, *99*, 7370–7371.
(25) It is important to recognize that if only one species is luminescent, the luminescence titration may not be a measure of pK_a^* (see ref 8).
(26) Forster, T. *Naturwissenschaften* **1949**, *36*, 186.
(27) Weller, A. *Prog. React. Kinet.* **1961**, *1*, 189–214.

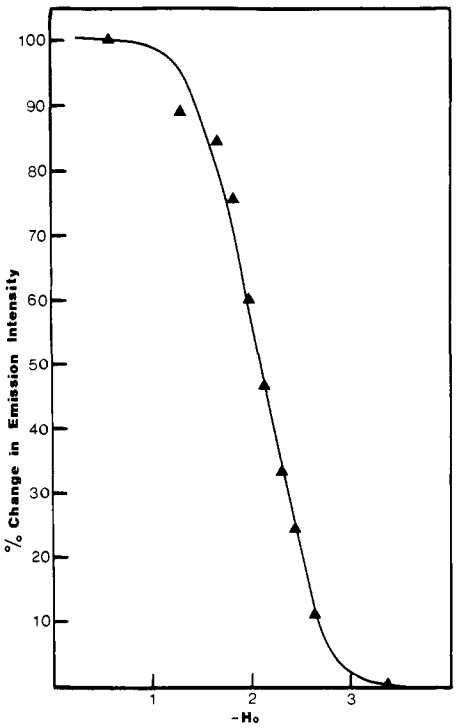

Figure 12. Luminescence titration curve of 1.4×10^{-5} M $Ru(bpz)_3^{2+}$ at ambient temperature in aqueous sulfuric acid solutions (18.9–49.8% H_2SO_4) with excitation and emission wavelengths set at 461 and 717 nm, respectively.

With the assumption that changes in entropy are minimal, one can derive eq 2[27] where T is the absolute temperature and ν_b and

$$pK_a^* = pK_a + (0.625/T)(\nu_b - \nu_a) \quad (2)$$

ν_a represent the (0–0) transition energy from ground to the relevant excited state (in cm^{-1}) for the base and acid forms, respectively. From eq 2, if ν_b is greater than ν_a, the base form will become a stronger base upon excitation. Conversely, if ν_a is greater than ν_b, the acid form will become stronger acid upon excitation. Since the (0–0) transition is not well-defined in this case, an approximation[19] is necessary. One such approximation, if the mean of the spectra shifts in emission are taken, results in the calculated pK_a^* values shown in Table III. There is generally poor agreement with experimentally determined values. Other authors[19,21,23] have found similar results when comparing calculated to experimental pK_a^* and have ascribed the errors to their inability to obtain a reasonable approximation for the relative difference in (0–0) transition energies between acid and base forms.

Figure 10A shows the effect of the excited-state protonation equilibrium in 18.9–48.9% sulfuric acid between $Ru(bpz)_2(Hbpz)^{3+}$ and $Ru(bpz)(Hbpz)_2^{4+}$ on their emission spectra. The corresponding luminescence titration curve is shown in Figure 12. Taking the inflection point of the curve in Figure 12 together with the lifetimes of $Ru(bpz)_2(Hbpz)^{3+*}$ and $Ru(bpz)(Hbpz)_2^{4+*}$ (see Table IV) and substituting them into eq 1 gives $pK_{a_2}^* = -2.4$. Since $pK_{a_2} = -3.0$, this represents an increase in the basicity of the excited state by 0.6 H_0 units. In 48.9–55% sulfuric acid, the emission band position and intensity do not change significantly even though in the ground-state $Ru(bpz)(Hbpz)_2^{4+}$ is being protonated to form $Ru(Hbpz)_3^{5+}$. This suggests that there is little difference between $Ru(bpz)(Hbpz)_2^{4+*}$ and $Ru(Hbpz)_3^{5+*}$ emissions, making it extremely difficult to calculate $pK_{a_3}^*$ with confidence.[28] Not surprisingly and in line with our model, the enhancement of basicity in the excited state is less in the second than in the first protonation step and not even observable in the third protonation step. Figures 10B and 11A,B show the emission

(28) Another possibility is that $pK_{a_2}^*$ and $pK_{a_3}^*$ lie too close together to be distinguishable. This seems unlikely since the corresponding ground-state pK_a values are readily distinguishable.

spectra as a function of acidity in the four to six protonation step region. Although the absorption spectra in this region (Figures 5B and 6) are not compellingly indicative of three species, combined with the emission data which clearly show three regions of emission with different lifetimes (Table IV), the data do seem most readily interpreted in terms of the fourth, fifth, and sixth protonation equilibria.

We know from Figures 5B and 6A,B the visible MLCT band blue shifts. Therefore, we expect, using eq 2, the excited states of $Ru(Hbpz)_2(H_2bpz)^{6+}$, $Ru(Hbpz)(H_2bpz)_2^{7+}$, and $Ru(H_2bpz)_3^{8+}$ to have enhanced acidity. The graphical analysis of the MLCT absorption data in Figures 5B and 6A shows the fourth and fifth protonation steps to overlap. The emission spectra of $Ru(Hbpz)_2(H_2bpz)^{6+}$ and $Ru(Hbpz)(H_2bpz)_2^{7+}$ also overlap as shown in Figures 10B and 11A. Because of this, it is not possible to calculate pK_{a_4}* and pK_{a_5}* without a more detailed analysis of both the ground- and excited-state protonation data. Nevertheless, the emission maxima and excited-state lifetimes are reported in Table IV.

Figure 11B shows the growth of $Ru(H_2bpz)_3^{8+}$ emission from 76.3 to 100% sulfuric acid. The background emission intensity particularly in 100% H_2SO_4, between 550 and 500 nm, is the tail end of solvent emission which decreases to negligible intensity at 620 nm. If we assume an excited-state equilibrium exists between $Ru(Hbpz)(H_2bpz)_2^{7+}$ and $Ru(H_2bpz)_3^{8+}$, with very little contribution from $Ru(Hbpz)_2(H_2bpz)^{6+}$, it is possible to calculate pK_{a_6}*. This assumption is reasonable since the final ground-state protonation step has been shown by graphical analysis to involve only two species, presumably $Ru(Hbpz)(H_2bpz)_2^{7+}$ and $Ru(H_2bpz)_3^{8+}$. The luminescence titration curve from the data associated with Figure 11B is shown in Figure 8. When the inflection point of the curve in Figure 8 together with the lifetimes of the species in excited-state equilibrium are substituted into eq 1, this gives pK_{a_6}* = −7.9. Since the ground-state pK_{a_6} = −6.7, this represents an increase in the acidity of the excited state by −1.2 H_0 units. Note that this result, obtained from lifetime analysis, is experimentally independent of the observation of an excited-state transition energy blue shift in the formation of this species.

The result is also consistent with the prediction that the excited states involving two protons per ligand would be more acidic than the ground state.

Summary and Conclusions

The combined weight of the absorption and emission data provide compelling evidence for the sequential hexaprotonation of the $Ru(bpz)_3^{2+}$ cation. This species would have a formal octapositive charge, which is exceptionally high outside the protein regime. Ion pairing in solution will undoubtedly minimize the effects of this high charge.

Although solvatochromism can lead to marked changes in spectra as the medium or pH is altered, the well-defined and predictable behavior of species II in acid medium suggests that solvatochromism does not make a significant contribution to our data. The identification of six processes occurring as the acidity is increased is most reasonably associated with the six available nitrogen atoms without complicating the situation further.

The simplicity of the spectrum in concentrated sulfuric acid should not be underemphasized since only when six protons have been added can the initial D_3 symmetry of the unprotonated species be recovered.

The pK_a and pK_a* values derived from the data and shown in Table III are totally consistent with the model initially envisaged and further support our sequential protonation premise. We feel bound to express this point most positively in view of the skepticism with which the idea of an octapositive cation has been met in our discussions of this system. It should be pointed out that such high formal charges are also found in well-known systems such as the protonated polyamines (polyamine hydrochlorides, etc.) or aggregated polysulfonated phthalocyanines and that our system only exists in the extreme environment of concentrated sulfuric acid. Since the data show that the free ligand bpz also readily picks up two protons, we should not be surprised when cation II picks up six.

The first three protonation steps involve nitrogen atoms, one on each coordinated ligand, which in the excited state are more basic than the ground state, the difference decreasing with each protonated step. Thus, in general, excitation results in an excited state which is quenched by reaction with a proton during its lifetime, i.e., the excited state, under the given acid conditions, contains at equilibrium one more proton than the ground state. The subsequent three protonation steps (four, five, and six) take place at a ligand which already possesses a proton and at a nitrogen atom which is less basic than the ground state. In general, excitation results in an excited state which tends to release a proton during its lifetime. A detailed study of the rates of these various processes is underway using laser pulse methods.[29] Note that in the Demas $Ru(bpy)_2(CN)_2$ system protonation occurs at the cyanide groups. When the complex is excited, charge is transferred to the bpy group formally leaving a Ru(III) bound to cyanide. Thus the excited state is a much stronger acid than the ground state; the protonated species lose their protons in the excited state and emission occurs from the excited unprotonated species.[3]

The excitation spectra for the variously protonated emitting states are similar to their absorption spectra but show pronounced structure and tend to be slightly red shifted of absorption. A referee has pointed out that we cannot be sure that the emitting states are MLCT for all the protonated species and that, because of their short lifetimes, some might be dd* in origin. Preliminary low-temperature studies to attempt to distinguish MLCT from dd emitting states led to the observation that for a given acid solution, the degree of protonation apparently increases with decreasing temperature. The question of the significance of the excitation spectra and the temperature phenomena will be the subject of a future publication.[30] We have also undertaken protonation experiments with the complexes $M(CO)_4bpz$ (M = Mo, W) where the presence of only one bpz ligand provides for an easier analysis.[31]

Our interest in the bipyrazine species (II) is in the design of highly photooxidizing photocatalysts, and it is pertinent that the redox couples associated with $Ru(bpy)_3^{2+}$ do shift positively in sulfuric acid by a significant amount as anticipated.[32] Resonance Raman work[33] is in hand[34] to provide further evidence for the structures of these species.

Acknowledgment. This research is part of a joint project with Prof. A. J. Bard (University of Texas at Austin), sponsored by the Office of Naval Research (Washington, DC), to whom we are indebted. We also thank the Natural Sciences and Engineering Research Council (Ottawa, Canada) for financial support and a postgraduate scholarship for R.J.C. We also appreciate the helpful criticism of Prof. Alan Hopkinson (York).

Registry No. II, 75523-96-5; DPZ, 10199-00-5.

(29) Crutchley, R. J.; Lever, A. B. P.; Kress, N., work in progress.
(30) Crutchley, R. J.; Lever, A. B. P., to be submitted for publication.
(31) Crutchley, R. J.; Eryavec, G.; Lever, A. B. P., submitted for publication.
(32) Bard, A. J.; Lever, A. B. P.; Crutchley, R. J., work in progress.
(33) Balk, R. W.; Stufkens, D. J.; Crutchley, R. J.; Lever, A. B. P. *Inorg. Chim. Acta* **1982**, *64*, L49–50.
(34) Dallinger, R. F.; Woodruff, W. H.; Lever, A. B. P.; Crutchley, R. J., work in progress.